RESEARCH ON SIMPLIFIED MAGNETIC FIELD MODEL AND TRANSMISSION CHARACTERISTICS OF PERMANENT MAGNET SCREW-NUT PAIRS

Junyue YANG[1], Xiaofan YE[1]*, Haitao LI[2,3], Yanjun GE[1]

The spiral structure of a permanent magnet screw-nut pairs makes its magnetic field coupling complicated, and the transmission characteristic is difficult to determine. The paper proposes a simplified method that can convert the 3D multi-pole spiral magnetic field of the permanent magnet screw-nut structure into a unipolar 2-D parallel plane magnetic field. The mathematical expressions of the axial magnetic thrust and the magnetic torque are obtained using an analytical method, which expresses the transmission characteristics and the relation between helix angle, pitch, screw diameter, and permanent magnet material parameters. The simulation results of a FEM 3D model by Ansys Maxwell software are in good agreement with the calculation results of the simplified model, verifying the effectiveness and feasibility of the simplified model.

Keywords: Permanent Magnet Screw-nut Pairs; Magnetic coupling; Magnetic field model optimization; Axial magnetic thrust; Transmission characteristics.

1. Introduction

The linear motion is widely used in modern industry, involving manufacturing, energy conversion, medical equipment, aerospace and many other fields [1, 2]. Traditionally, linear motion is obtained mainly by using mechanical mechanisms such as screw-nut pairs. However, as mechanical contact and friction between the moving parts are inevitable, problems such as stuck, wear, or large vibrations, may occur [3].

The permanent magnet screw-nut pairs is a new type of magnetic transmission device. It is a transmission that converts the rotational motion of the motor into a linear motion, using a contactless motion between a permanent magnet screw and a permanent magnet nut. Based on magnetic field coupling between the parts, it avoids the disadvantages of mechanical screw jamming, wear or vibration, and it has the advantages of no contact, no friction, no wear, has a simple structure,

[1] School of Mechanical Engineering, Dalian Jiaotong University, Dalian, Liaoning, 116028, China, email: fye951809@gmail.com (corresponding author)
[2] CRRC Zhuzhou Locomotive Co., Ltd, Zhuzhou, 412001, China, email: 504703997@qq.com
[3] The Hunan Key Laboratory of Maglev Transportation Vehicle System Integration, Zhuzhou, 412001, China, email: 504703997@qq.com

and provides overload protection [4, 5]. These justified the scholars interest, who researched this technology and achieved certain achievements.

To study the permanent magnet screw-nut pairs, Gao et al. used a 3-D analytical model to predict the magnetic field distribution and electromagnetic performance of a magnetic screw [6]. Liu et al. studied the design of a magnetic screw by using 2-D and 3-D finite element models [7]. Gao et al. analyzed the thrust characteristics of a magnetic screw using a 2-D finite element model [8]. Mustafa et al. reviewed the work of a magnetic screw and listed a method to calculate the thrust [9]. Wang et al. proposed an analysis method based on a magnetic field solution to calculate the thrust of the magnetic screw system and performed 2-D and 3-D finite element analysis [10].

Based on the above-quoted literature, it can be concluded that most of the existing research is based on numerical modeling using the finite element method, to study the magnetic thrust characteristics of permanent magnet screw-nut pairs. However, the spiral structure of the magnetic field makes magnetic field circuit to be distributed in both axial and cross sections, with mutual coupling effects. Most current models are 2-D or 3-D finite element models established by simulation software, which cannot clearly express transmission performance and relation between parameters. This paper proposes a model simplified method for the helical magnetic field, and mathematical expressions of axial magnetic thrust and magnetic torque are derived by analytical method, which visually expresses transmission characteristics of permanent magnet screw-nut pairs. Furthermore, the 3-D simulation model of permanent magnet screw-nut pairs is established base on Ansys Maxwell. And the simplified mathematical model has good consistency with the 3-D simulation model by comparison.

2. Structure and principle

Fig. 1 is the basic structure of the permanent magnet screw-nut pairs.

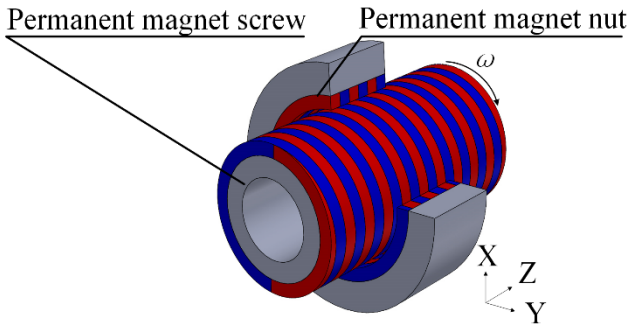

Fig. 1. Basic structure of the permanent magnet screw-nut pairs

In Fig. 1, the permanent magnet screw-nut pairs is mainly composed of permanent magnet screw and permanent magnet nut. The permanent magnet screw is composed of an internal core and an external spirally arranged permanent magnet, and the permanent magnet nut is composed of an external core and an internal spirally arranged permanent magnet. The two parts of permanent magnets are composed of permanent magnet spiral strips with opposite N-S poles, and spiral angles are same. There is a uniform air gap between the inner and outer permanent magnets. The permanent magnet screw is capable of rotating along the central axis under the drive of a rotary electric motor, whereas the permanent magnet nut can only perform linear motion along the axial direction.

In Fig. 2, in static and no-load state, according to the principle of minimum air gap reluctance, the N-S poles of inner and outer permanent magnets are aligned. In this state, the magnetic force is a radial force without an axial force component.

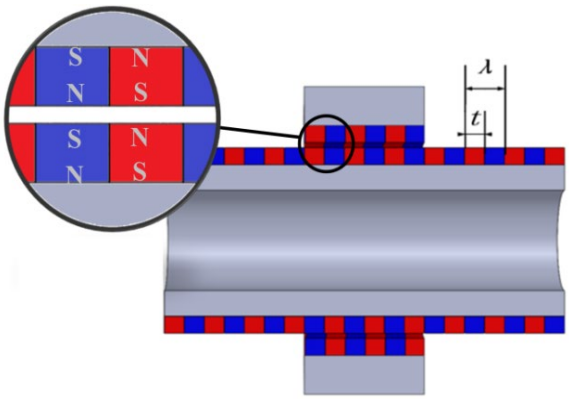

Fig. 2. Relative position of magnetic pole in static and no-load state

In Fig. 3, under the rotation or load state of the permanent magnet screw, the relative position between inner and outer permanent magnet blocks will shift due to spiral structure of permanent magnet block. In this state, the magnetic force between permanent magnets will generate an axial component, which drives the permanent magnet nut to perform axial linear motion.

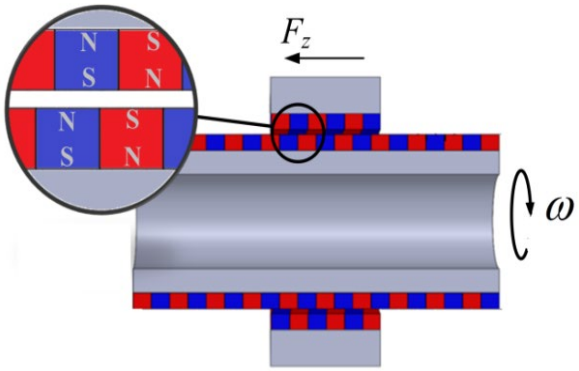

Fig. 3. Relative position of magnetic pole in rotating or load state

According to Fig. 1 to Fig. 3, the permanent magnet screw-nut pairs can realize conversion from rotational motion to linear motion by air gap magnetic field without contact. Under the condition that the permanent magnet screw rotates with angular velocity ω and permanent magnet nut moves at a linear speed v, the transmission relation can be expressed as:

$$\omega=2\pi\frac{v}{\lambda}=\pi\frac{v}{t} \tag{1}$$

where λ is the pitch of the permanent magnet screw, t is the axial length of the unipolar permanent magnet. $\lambda=2t$, which is shown in Fig. 2.

The transmission ratio of the magnetic screw can be expressed as Eq. (2).

$$G=\frac{\omega}{v}=\frac{2\pi}{\lambda} \tag{2}$$

3. Establishing the magnetic field simplified model

In Fig. 3, in load state, there is a shift between the magnetic field on the outer side of the screw and the magnetic block field on the inner side of nut. Due to its spiral structure, the magnetic field circuit is distributed in both the axial section and cross section, which affects and couples with each other. The distribution of the magnetic field is complex, and it is difficult to represent its distribution by 2-D plane. The calculation and analysis are also complicated. Based on its structure and operation principle, this paper deconstructs coupled magnetic field and establishes a simplified magnetic field model that is easy to analyze.

According to position of magnetic pole in static and no-load state shown in Fig. 2, the spiral structure is shown in Fig. 4a. It can be deconstructed into a set of N-S magnetic strips and expand along a fixed angle, as shown in Fig. 4b.

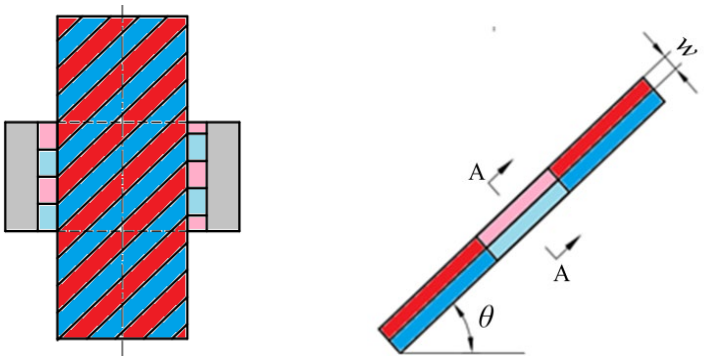

a. Spiral structure b. Expanded spiral structure

Fig. 4. Magnetic pole expansion in static and no-load conditions

In Fig. 4, θ is the helix angle, w is the width of the permanent magnet block along the direction perpendicular to the helix angle, $w=t\sin\theta$.

In Fig. 4, by transforming the spiral magnetic pole into a linear magnetic pole and transforming the spiral magnetic field coupling relation into a linear correspondence, the correspondence between the internal and external magnetic fields of the permanent magnet screw-nut pairs is obvious.

Similarly, Fig. 5 is the result of expanding the magnetic pole position in the rotating or load state shown in Fig. 3.

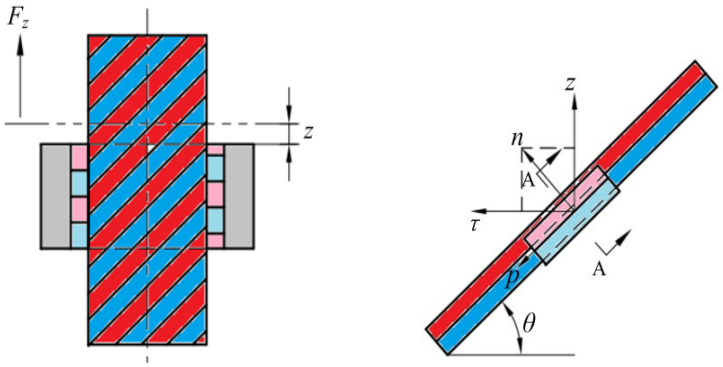

a. Spiral structure b. Expanded spiral structure

Fig. 5. Magnetic pole deployment in rotating or load state

In Fig. 5a, the axial magnetic pole position shift is z ($z\leq t$). An axial magnetic force is generated due to the displacement of center position of the corresponding permanent magnet blocks. In Fig. 5b, there is a z-τ ordinate system, z is the axial direction and τ is the tangential direction of the circle.

In Fig. 4 and Fig. 5, the A-A cross section is perpendicular to the helix angle, and the n-p coordinate system can be established on the A-A cross section. n is the

vertical direction along the helix angle, p is the direction of the spiral magnetic pole, and the angle between the n axis and the z axis is θ, $n=z/\cos\theta$.

Fig. 6 and Fig. 7 show the distribution of magnetic field loop and the magnetic field line through the A-A cross section of Fig. 4 and Fig. 5.

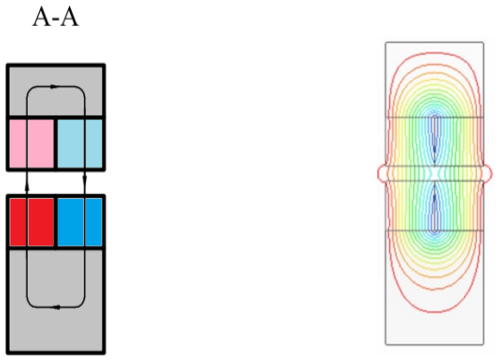

a. Magnetic flux loop b. Distribution of magnetic induction lines

Fig. 6. Distribution of magnetic flux loop and magnetic induction line under no-load condition

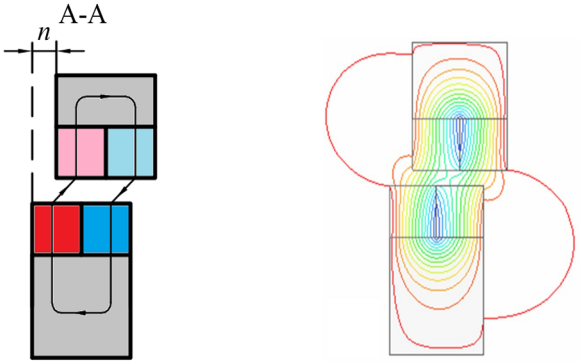

a. Magnetic flux loop b. Distribution of magnetic induction lines

Fig. 7. Distribution of magnetic flux loop and magnetic induction line under load condition

In Fig. 6 and Fig. 7, the spiral magnetic field coupled by multipole pairs is transformed into a simple 2-D parallel plane magnetic field by magnetic field deconstruction. When the structural parameters are determined, the distribution of the magnetic field is only determined by one parameter n. So a simplified magnetic field model is established.

The relation between the magnetic field and the displacement can be visually displayed by the simplified magnetic field model shown in Fig. 4 to Fig. 7, and it can be solved directly by analytical method. The axial magnetic thrust and magnetic torque can be further derived.

4. Calculation of magnetic thrust and magnetic torque

The air gap magnetic field is energy conversion area of the permanent magnet screw-nut pairs. From the distribution of the magnetic induction lines in Fig. 6b and Fig. 7b, the air gap magnetic field changes significantly under different load conditions. Therefore, this paper mainly takes the air gap magnetic field as the research object, and derives the mathematical expressions of magnetic thrust and magnetic torque.

In the simple 2-D parallel plane magnetic field shown in Fig. 6 and Fig. 7, the air gap magnetic field coordinate system is established with a magnetic angle of 2π from one N-S pole pairs, and the magnetomotive force of the permanent magnet is transformed into the fundamental wave of the magnetomotive force on the air gap surface by Fourier transform. Fig. 8 shows the distribution curve of the fundamental wave of the magnetomotive force on the surface of the air gap magnetic field.

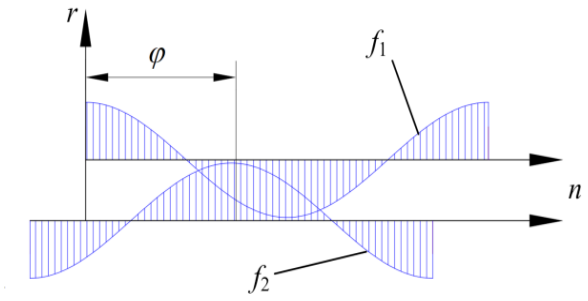

Fig. 8. Magnetic field distribution in air gap

In Fig. 8, r is the radial direction of the permanent magnet screw, φ is the magnetic angle, f_1 and f_2 are the magnetomotive force fundamental waves of the permanent magnet nut and the permanent magnet screw in the air gap, respectively, and Φ is the phase difference caused by the magnetic pole misalignment.

$$\Phi = \frac{\pi}{2} - \frac{n}{w}\pi = \frac{\pi}{2} - \frac{z}{t}\pi \tag{3}$$

The fundamental magnetomotive force can be expressed as:

$$\left.\begin{aligned} f_1 &= F_1 \cos(\varphi), \quad r = R_1 \\ f_2 &= F_2 \cos(\varphi - \Phi), \quad r = R_2 \end{aligned}\right\} \tag{4}$$

where R_1 is the inner radius of the permanent magnet nut, R_2 is the outer radius of the permanent magnet screw. F_1 and F_2 are the fundamental amplitude of the permanent magnet magnetomotive force, which can be expressed as:

$$F_1 = F_2 = \frac{4}{\pi} H_c l_c \tag{5}$$

where H_c is the residual magnetic field strength of the working point of the permanent magnet, l_c is the magnetization thickness of the permanent magnet.

The magnetic vector potential A is introduced as the solution variable. Since Fig. 8 is a 2-D plane field, it is only necessary to solve the scalar Laplace equation in the p direction, as shown in Eq. (6).

$$\frac{\partial^2 A_p}{\partial r^2} + \frac{1}{r}\frac{\partial A_p}{\partial r} + \frac{1}{r^2}\frac{\partial^2 A_p}{\partial \varphi^2} = 0 \tag{6}$$

The boundary conditions of the air gap magnetic field are shown in Eq. (7):

$$\left.\begin{aligned} H_\varphi(r,\varphi)_{r=R_1} &= f_1 \\ H_\varphi(r,\varphi)_{r=R_2} &= f_2 \end{aligned}\right\} \tag{7}$$

By using the method of separating variables to solve Eq. (6), it can be obtained that:

$$A_p = \frac{\mu_0 (r + r^{-1}R_2^2)}{(R_1^2 - R_2^2)R_1^{-2}} F_1 \cos(\varphi) + \frac{\mu_0 (r + r^{-1}R_1^2)}{(R_1^2 - R_2^2)R_2^{-2}} F_2 \cos(\varphi - \Phi) \tag{8}$$

where μ_0 is the magnetic permeability of air, and $\mu_0 = 4\pi \times 10^{-7}\,\mathrm{T} \times \mathrm{m} \times \mathrm{A}^{-1}$.

The magnetic field intensity component in the air gap can be expressed as:

$$\left.\begin{aligned} H_\varphi &= -\frac{1}{\mu_0}\frac{\partial A_p}{\partial r} = -\frac{r + r^{-1}R_2^2}{(R_1^2 - R_2^2)R_1^{-2}} F_1 \cos(\varphi) - \frac{r + r^{-1}R_1^2}{(R_1^2 - R_2^2)R_2^{-2}} F_2 \cos(\varphi) \\ H_r &= -\frac{1}{\mu_0}\frac{\partial A_p}{\partial \varphi} = \frac{r + r^{-1}R_2^2}{(R_1^2 - R_2^2)R_1^{-2}} F_1 \sin(\varphi - \Phi) + \frac{r + r^{-1}R_1^2}{(R_1^2 - R_2^2)R_2^{-2}} F_2 \sin(\varphi - \Phi) \end{aligned}\right\} \tag{9}$$

The magnetic field energy in the air gap can be expressed as Eq. 10:

$$W_m = \frac{1}{2}\mu_0 \iiint_V (H_r^2 + H_\varphi^2) d\varphi dr dp \tag{10}$$

where V is the volume of the air gap. The electromagnetic thrust in the n direction can be expressed as:

$$F_n = \frac{1}{R_2}\frac{\partial W_m}{\partial \Phi} = -\frac{32\mu_0 L_p l_c^2}{\pi}\frac{R_1^2 R_2}{R_1^2 - R_2^2} H_c^2 \cos\Phi \tag{11}$$

In Eq. (5), L_p is the length of the permanent magnet nut after the magnetic pole is expanded, and its relation with the axial length of the nut is $L_p = L_s/\sin\theta$.

According to Eq. (5), the axial magnetic thrust and the magnetic torque along the circumferential direction of the permanent magnet screw-nut pairs can be expressed as:

$$\left.\begin{aligned} F_z &= F_n \cos\theta = -\frac{32\mu_0 L_p l_c^2}{\pi}\frac{R_1^2 R_2}{R_1^2 - R_2^2} H_c^2 \cos\theta \sin\left(\frac{z}{t}\pi\right) \\ T_e &= F_n \sin\theta R_2 = \frac{32\mu_0 L_p l_c^2}{\pi}\frac{R_1^2 R_2^2}{R_1^2 - R_2^2} H_c^2 \sin\theta \sin\left(\frac{z}{t}\pi\right) \end{aligned}\right\} \tag{12}$$

Based on Eq. (12), under the condition that the basic structural parameters are determined, the magnetic thrust and magnetic torque are determined by the offset distance n. When n changes with the load or rotation of the permanent magnet screw-nut pairs, the magnetic thrust and magnetic torque change with the sine function relation respectively. When $n=w/2$, the magnetic thrust and magnetic torque reach the peak.

The H_c in Eq. (12) is determined by the working point of permanent magnet. In this paper, NdFeB35 is used as the permanent magnet material. Fig. 9 shows the hysteresis loop of NdFeB35.

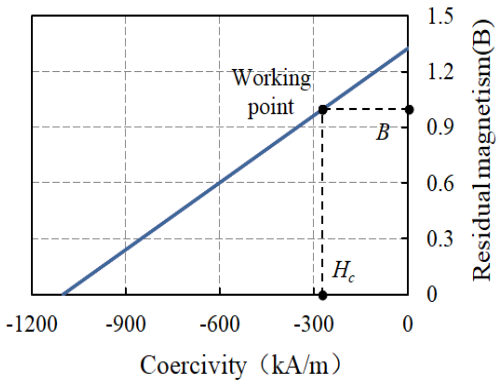

Fig. 9. Demagnetization curve of permanent magnet block

When the permanent magnet screw-nut pairs is running, the working point of the permanent magnet also changes with the difference of the offset distance n. The working point changes along the curve shown in Fig. 9. When using Eq. 12 to calculate the magnetic thrust, it is necessary to assume a working point first, and then use the iterative solution of Eq. 9 to correct the assumed working point.

5. Simulation analysis and comparison

Based on the relation between parameters of magnetic lead screws[7], the 3-D simulation model of permanent magnet screw is established by using Ansys Maxwell software. The specific parameters are shown in Table 1 and Table 2.

Table 1

Material parameters of magnetic screw-nut pairs

Paramrter	Value
Material of screw iron core	Q235
Material of permanent magnet on the screw	NdFe35
Material of the iron core on the nut	Q235
Material of permanent magnet on the nut	NdFe35

Table 2

Structural parameters of permanent magnet screw-nut pairs

Paramrter	Value
Inner diameter of screw(mm)	29.5
Outer diameter of screw(mm)	54.5
Inner diameter of nut(mm)	90.5
Outer diameter of nut(mm)	57.5
Axial length of nut(mm)	30
Spiral angle of rise of permanent magnet(deg)	10.40
Axial width of permanent magnet(mm)	5
Radial thickness of permanent magnet(mm)	5

Based on the parameters in Table 1 and Table 2, a 3-D FEA model of permanent magnet screw-nut pairs is established by the Ansys Maxwell software as shown in Fig. 10.

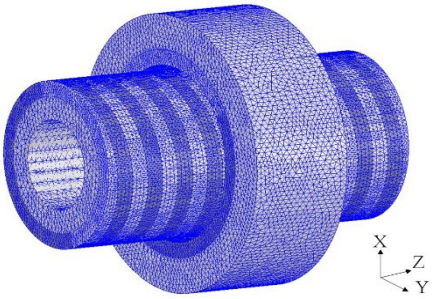

Fig. 10. 3-D FEA model

The geometric model is shown in Fig. 10, the material properties of each component are defined and allocated according to Table 1 and Table 2. The excitation source is the magnetic field provided by the permanent magnet, and the mesh division of the iron core and permanent magnet block is set to a single maximum mesh length of 2.5mm. The mesh division of the permanent magnet block is set to a single maximum mesh length of 1.5mm. The mesh division in the air gap is more refined, with a maximum length of 1mm for a single mesh. The permanent magnet screw part is selected as the body domain that requires computational force. Fig. 11 shows the simulation results of 3-D FEA model magnetic field distribution.

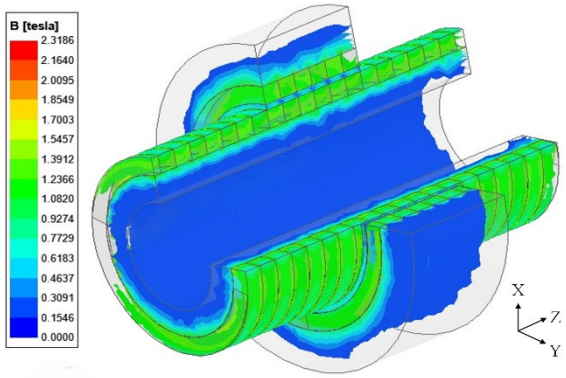

Fig. 11 Magnetic field distribution of 3-D model

By adjusting the corresponding position of the magnetic pole between the permanent magnet screw and the permanent magnet nut, the magnetic induction line and the magnetic induction intensity distribution chart along the axial section are obtained, as shown in Fig. 12 and Fig. 13.

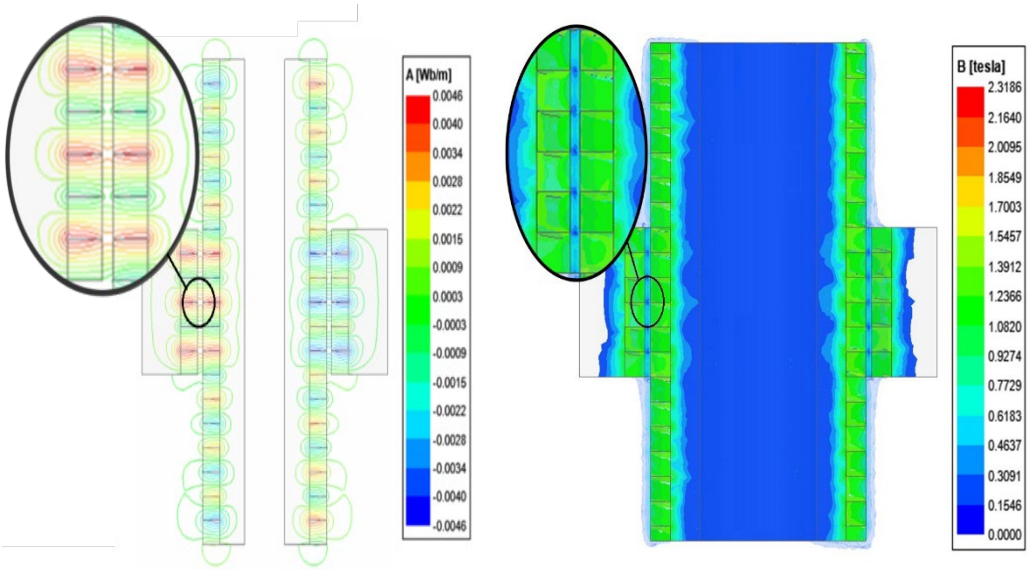

a. Magnetic induction line distribution b. Magnetic induction intensity distribution

Fig. 12. Magnetic field distribution in no-load state

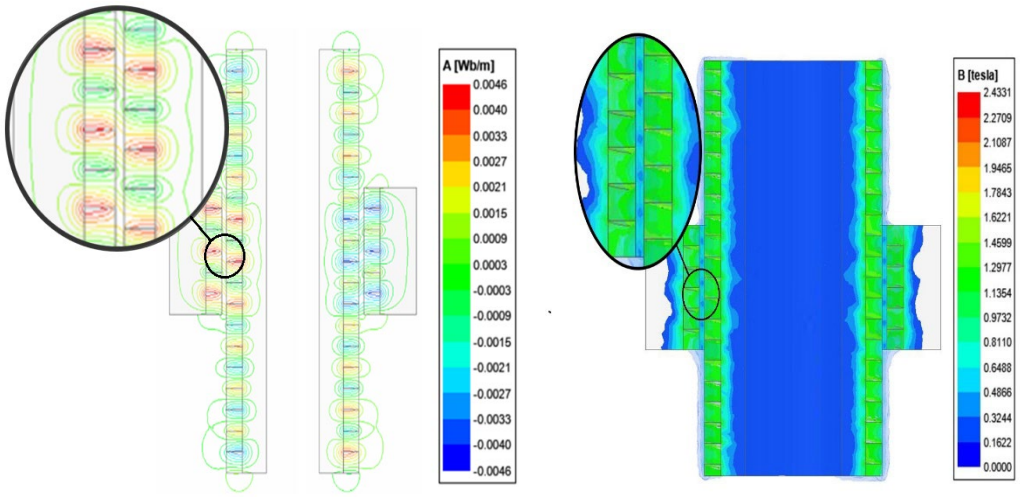

a. Magnetic induction line distribution b. Magnetic induction intensity distribution

Fig. 13. Magnetic field distribution when the magnetic thrust is at its peak

Fig. 12 and Fig. 13 are the magnetic induction line and magnetic induction intensity distribution nephogram of the axial section of the permanent magnet screw under the no-load state (n=0) and the maximum axial load (n=w/2), respectively. By comparison, the average magnetic induction intensity (0.97T) of the air gap under load is slightly higher than that under no-load (0.92T). This is because the air gap magnetic field under no-load has only radial component, while under load, the air gap magnetic field produces axial component. The magnetic induction line also produces deformation, and the magnetic attraction direction is along the axial direction.

By changing the displacement distance z of the magnetic pole of the permanent magnet, the relation curve between the displacement deviation angle ($z\pi/t$) of the magnetic pole in the period and the axial magnetic thrust can be obtained. The results of the curve are compared with the simplified model calculation results of the axial magnetic thrust calculated by Eq. (12), as shown in Table 3.

Table 3

Simplified model and 3-D model magnetic thrust results

Displacement deviation angle /deg	Simplified model for calculating thrust /N	3D model simulation thrust /N
0	0	0
18	99.426	174.534
36	229.537	332.963
54	385.976	456.312
72	524.319	537.162
90	607.665	564.805

108	615.711	536.734
126	548.632	457.237
144	413.765	332.675
162	225.242	174.304
180	0	0
198	-225.146	-174.535
216	-413.775	-331.984
234	-548.585	-456.937
252	-614.120	-537.037
270	-612.212	-564.805
288	-527.111	-536.936
306	-387.769	-455.987
324	-231.886	-332.203
342	-99.236	-174.607
360	0	0

The relation curve between magnetic thrust and displacement deviation angle obtained from Table 3 is shown in Fig. 14.

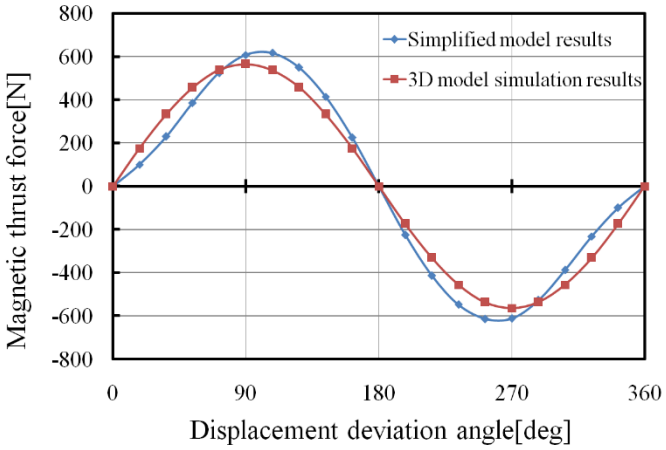

Fig. 14. Relation between magnetic thrust and displacement deviation angle

In Fig. 14, the 3-D model simulation curve and the simplified model calculation curve are sinusoidal. The maximum error is 8.72%, but the simulation value of the magnetic thrust is lower than simplified model calculation value. This is because in the simplified process of the magnetic field model, the coupling magnetic field of multi-stage pairs is simplified to a 2-D plane magnetic field with only one magnetic pole pairs. There is more boundary magnetic flux leakage, but it is not considered in theoretical calculation process, while the influence of boundary magnetic flux leakage is considered in simulation process. In general, the simplified model calculation curve and the 3-D model simulation curve have good

consistency. The 3-D model simulation results verify the feasibility of the magnetic field model simplified and theoretical derivation equation.

6. Conclusions

The simplified method proposed in this paper simplifies the magnetic field model of the permanent magnet screw-nut pairs. The spiral complex coupling magnetic field is derived by using only one pole-pairs plane magnetic field model, which reveals the characteristics of the magnetic field change during operation of the permanent magnet screw-nut pairs. This model also shows the relation between the axial magnetic thrust and the magnetic pole displacement, and considers the displacement of the permanent magnet working point with different working states. Finally, the iterative calculation method is given by these conditions. However, the simplified model has only one magnetic pole pairs, and there is more boundary magnetic flux leakage. In further research work, it is necessary to modify the calculation process according to the experimental results.

REFERENCES

[1]. *S. Guo, Z. Wang, Q. Fu*, Motion Performance evaluation of a Magnetic Actuated Screw Jet Microrobot, 2017 IEEE International Conference on Mechatronics and Automation (ICMA), pp. 2000-2004, 2017.

[2]. *F. Xiao, Y. Du, Y. Wang, M. Chen, T. W. Ching and X. Liu*, "Modeling and Analysis of a Linear Stator Permanent-Magnet Vernier HTS Machine", in IEEE Transactions on Applied Superconductivity, **vol. 25**, no. 3, 2015, pp. 1-4.

[3]. *M. Hanifzadegan, R. Nagamune*, Tracking and Structural Vibration Control of Flexible Ball–Screw Drives with Dynamic Variations, IEEE/ASME Transactions on Mechatronics, **vol. 20**, no. 1, 2015, pp.133-142.

[4]. *Z. Ling, J. Ji, J. Wang, W. Zhao*, Design Optimization and Test of a Radially Magnetized Magnetic Screw with Discretized PMs, IEEE Transactions on Industrial Electronics, **vol. 65** 1984. no. 90, 2018, pp. 7536-7547.

[5]. *J. Ji, Z. Ling, J. Wang, W. Zhao, G. Liu and T. Zeng*, Design and Analysis of a Halbach Magnetized Magnetic Screw for Artificial Heart, IEEE Transactions on Magnetics, **vol. 51**, no. 11, Nov. 2015, pp. 1-4.

[6]. *F. Gao, Q. Wang, J. Zou*, Analytical Modeling of 3-D Magnetic Field and Performance in Magnetic Lead Screws Accounting for Magnetization Pattern, IEEE Transactions on Industrial Electronics, **vol. 67**, no. 6, 2020, pp. 4785-4796.

[7]. *X. Liu, Y. Liu, X. Li*, Parametric Analysis and Design of Magnetic Lead Screw, 2019 IEEE International Electric Machines & Drives Conference (IEMDC), 2019, pp. 1990-1995.

[8]. *F. Gao, Q. Wang, Y. Xu, J. Zou*, Analysis of an inductor magnetic lead screw, 2017 IEEE Transportation Electrification Conference and Expo, Asia-Pacific (ITEC Asia-Pacific), 2017, pp. 1-4.

[9]. *D. Mustafa, H. A. Hussain*, A Survey on the Design and Analysis of Magnetic Screws, 2021 IEEE Energy Conversion Congress and Exposition (ECCE), 2021, pp. 3759-3766.

[10]. *J. Wang, K. Atallah, W. Wang*, Analysis of a Magnetic Screw for High Force Density Linear Electromagnetic Actuators, **vol. 47,** no. 10, 2011, pp. 4477-4480.